Heliyon 10 (2024) e35457

Contents lists available at ScienceDirect

Heliyon

journal homepage: www.cell.com/heliyon

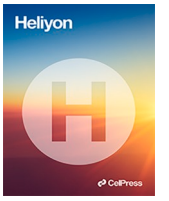

Research article

MiR-93-5p inhibits ovarian cancer through SLC7A11-mediated-ferroptosis

Chunxia Li [b,1], Zitao Wang [a,1], Yanqing Wang [a], Hua Liu [a,*], Yanxiang Cheng [a,**]

[a] Department of Obstetrics and Gynecology, Renmin Hospital of Wuhan University, Wuhan, Hubei, China
[b] Department of Obstetrics and Gynecology, Wuhan Wuchang Hospital, Wuhan, Hubei, 430065, China

ARTICLE INFO

Keywords:
miR-93-5p
Ovarian cancer
SLC7A11
Ferroptosis
Erastin

ABSTRACT

Aim: Ovarian cancer (OC) is the most lethal gynecological malignancy, which seriously affects the prognosis and life quality of female patients. Therefore, new therapeutic targets and treatments are urgently needed.

Methods: Expression levels of miR-93-5p and SLC7A11 and ferroptosis status in paracancerous and tumor tissues were examined and compared. The effect of the miR-93-5p-SLC7A11 regulatory loop on the malignant phenotype as well as the ferroptosis phenotype of SKOV3 cells was assessed. Furthermore, the interaction between miR-93-5p and SLC7A11 was confirmed via rescue experiment.

Results: In this study, we found that miR-93-5p was lowly expressed in cancer tissues, and suggested that overexpression of miR-93-5p could target SLC7A11 to reduce its expression and promote ferroptosis, thereby inhibiting the malignant biological behaviors such as proliferation, invasion and migration, while knockdown of miR-93-5p restrained ferroptosis and promoting tumor growth. Besides, erastin, as a specific inhibitor of SLC7A11, could target down the expression of SLC7A11, induce the occurrence of ferroptosis, and reverse the effect of knockdown of miR-93-5p.

Conclusions: Taken together, our findings disclosed that miR-93-5p increased the level of ferroptosis and inhibited the progression of OC by targeting and inhibiting the expression level of SLC7A11, which was a potential treatment in OC.

1. Introduction

Ovarian cancer (OC) is the malignant tumor with the highest mortality rate among female reproductive cancers worldwide, especially in China [1]. For most patients, the heterogeneity and ambiguity of symptoms leads to delayed and advanced diagnosis, with a low survival prognosis. Currently, the mainstream treatments for OC include surgery and platinum-based combination chemotherapy. Although patients initially respond sensitively to the therapy, most of them relapse due to drug resistance and disease recurrence, thus resulting the unsatisfactory five-year survival rate [2]. Therefore, it is of great significance to identify key predictive

* Corresponding author. No.99, Zhangzhidong Road, Wuchang, Wuhan, Hubei, 430065, China.
** Corresponding author. No.99, Zhangzhidong Road, Wuchang, Wuhan, Hubei, 430065, China.
E-mail addresses: 1532940649@qq.com (C. Li), 2020283020254@whu.edu.cn (Z. Wang), wangyq@whu.edu.cn (Y. Wang), liuhua008@tom.com (H. Liu), yanxiangCheng@whu.edu.cn (Y. Cheng).
[1] Chunxia Li and Zitao Wang contributed equally to this work.

https://doi.org/10.1016/j.heliyon.2024.e35457
Received 13 March 2024; Received in revised form 25 July 2024; Accepted 29 July 2024
Available online 30 July 2024

biomarkers and precise mechanisms to provide effective therapeutic strategies for treatments.

Ferroptosis, a novel iron-dependent programmed cell death, is characterized by iron accumulation, driven by lipid peroxidation [3]. Several previous studies have illustrated the involvement of microRNAs in various cancer pathological mechanism, including ferroptosis. Accumulating researches proved the indispensable role of ferroptosis in tumorigenesis, progression, and metastasis in multiple cancers, including OC [4,5]. In terms of SLC7A11, the gene functions to import cystine for glutathione biosynthesis and antioxidant defense, counteracts cellular oxidative stress and suppresses ferroptosis by maintaining cellular levels of GSH, a key pathway for redox homeostasis [6,7]. Besides, the overexpression of SLC7A11 has been detected in multiple malignant tumors, and regulates tumor development, proliferation, metastasis, microenvironment and therapy resistance, furtherlinked with poor prognosis and resistance [8]. However, its expression level, regulatory mechanism and role of ferroptosis regulation in OC remain unknown. Therefore, induction of ferroptosis is quite a prospective cancer strategy.

microRNAs (miRNAs) with a length of about 25 nt are small non-coding RNAs that regulate gene expression by binding to the 3'UTR of target mRNAs and play a pivotal role in cell biological behaviors such as differentiation, proliferation, and apoptosis [9,10]. Extensive studies have shown that miRNAs are promising diagnostic and prognostic molecular biomarkers as well as therapeutic targets for cancer [11,12]. miR-93-5p, which has been found to be differentially expressed in a variety of tumors, has also been shown to be closely related to the occurrence and development of tumors [13–15]. For example, Li et al. found that miR-93-5p promoted gastric cancer cell progression through inactivation of the Hippo signaling pathway [16], but the mechanism of miR-93-5p involved in the regulation of ferroptosis in OC was still unclear, and its role needed to be further studied. Furthermore, several recent studies have shown that downregulation of certain tumor suppressor miRNAs can make cancer cells highly susceptible to ferroptosis, which might provide new potential solutions for cancer treatment [17–19].

In our study, we found that miR-93-5p, as a tumor suppressor gene, could promote ferroptosis by inhibiting the expression of SLC7A11, thereby suppressing the malignant phenotype of OC cells, which might be an emerging target of OC, providing a new and promising insight for the targeted therapy in OC.

2. Materials and methods

2.1. Microarray data

The miRNA expression profiles were obtained from the GSE53829 dataset from the GEO database (14 normal samples and 45 cancer tissue samples). Besides, the mRNA expression profiles were downloaded from the GTEX and TCGA datasets and the two datasets were integrated to remove batch effects (88 normal tissues and 375 OC tissues).

2.2. Expression of ferroptosis-related genes

Ferroptosis-related genes were obtained from the FerrDb V2 database (http://www.zhounan.org/ferrdb/current/), including Driver, Suppressor and Marker genes. Based on the expression of these key genes, the GEPIA2 database (http://gepia2.cancer-pku.cn/#index) was utilized to detect the differential expression of ferroptosis-related genes in normal tissues and OC tissues.

2.3. Identification of differentially expressed genes (DEGs)

GEO2R, a freely accessible web platform (http://www.ncbi.nlm.nih.gov/geo/geo2r), was utilized to juxtapose gene expression profiles across various cohorts, thereby enabling the identification of differentially expressed genes (DEGs) and microRNAs (miRNAs) between tumor specimens and normal counterparts. A statistical significance threshold of P-value <0.05 was employed to highlight meaningful discrepancies.

2.4. Functional enrichment analysis

Based on the filtrated DEGs, GO and KEGG analysis was performed by the "clusterProfiler" package to identify the key functions and pathways in the occurrence and development. Meanwhile, the functional enrichment analysis of miRNAs and target genes was performed to explore the role of miRNAs in OC.

2.5. Tissue collection and ethics statement

Nine OC tissues and three normal tissues were collected from the People's Hospital of Wuhan University. All samples immersed in RNA post stabilization solution were kept in liquid nitrogen and stored at −80 °C. The study was approved by the Ethics Committee of the People's Hospital of Wuhan University, and participants signed a written informed consent (WDRY2020-K218).

2.6. Cell culture and transfection

Human normal ovarian cell line IOSE-80 and OC cells SKOV3 were obtained from China Center for Type Culture Collection (Wuhan, China). SKOV3 and IOSE-80 cells were cultured in RPMI1640 medium (Meilunbio, China) containing 10 % FBS (Gibco, Life Technologies, Grand Island, NY), 100 U/mL penicillin and 100 μg/mL streptomycin (Invitrogen, Waltham, MA, United States) at 37 °C.

5 % CO_2 incubator. This study used a set of lentiviruses overexpressed and knocked down by miRNA-93-5p (Genechem Co., LTD). SKOV3 cells (4×10^5 cells/well) were individually seeded into six-well plates, cultured in RPMI1640 containing 10 % FBS according to the manufacturer's instructions, and then transfected with NC, OE-miRNA-93-5p and SI-miRNA-93-5p lentiviruses with transfection agents. Forty-eight hours after infection, stably infected cells were selected with puromycin (Invitrogen, United States). Eventually, quantitative real-time PCR (qRT-PCR) or Western Blot verified the transfection efficiency.

2.7. qRT-PCR

In guide of the manufacturer's instructions, total RNA was isolated from cells or tissues using the Trizol reagent (Invitrogen), which was reverse transcribed using a reverse transcription kit (Yeasen Biotechnology Co. Ltd.), and qRT-PCR was conduct based on the resulting cDNA. On the basis of the manufacturer's instructions (Yeasen Biotechnology Co. Ltd.), gene expression quantification in triplicate was performed on a Bio-Rad PCR system using SYBR GREEN PCR Master Mix. The expression levels of SLC7A11 and miR-93a-5p were normalized with respect to GAPDH as the internal control for SLC7A11, and U6 for miR-93a-5p. The primers used are shown in the Supplementary Table 1. The $2^{-\Delta\Delta Ct}$ method was used to calculate the relative gene expression.

2.8. Western Blot

After treating with RIPA buffer containing protease and phosphatase inhibitors (Beyotime Institute of Biotechnology) for 30 min, total protein was extracted from collected tissues or cultured cells. Protein concentrations were measured by BCA protein assay kit (Beyotime Biotechnology, China). 10 μg of total protein lysates were electrophoresed in 10 % and 12.5 % SDS-polyacrylamide gels (Yeasen Biotechnology Co. Ltd.), and proteins separated in the gels were transferred to PVDF membranes (Merck Millipore, Billerica, MA). Block the membrane with 5 % milk blocking solution for 1 h at room temperature. Remove blocking solution and add diluted primary antibody overnight at 4 °C. Then, wash 3 times with TBST for 5 min each. The diluted secondary antibody was added, incubated at room temperature for 1 h, and washed 3 times with TBST at room temperature for 5 min each time. After freshly prepared ECL Enhanced Plus Kits (ABclonal, China), protein expression was detected by a chemiluminescence detection system (Bio-Rad, USA). Protein expression was analyzed using ImageJ software.

2.9. Cell counting Kit-8 assay (CCK-8)

CCK-8 assay was employed to detect the cell viability. Firstly, SKOV3 cells were seeded into 96-well plates (5×10^3 cells/well). After 3 consecutive days of culture, 10 μL of CCK-8 reagent (Glpbio technology, China) was added to each well, and the cells were incubated in a 37 °C atmospheric incubator with 5 % CO2 for another 2 h. Finally, the absorbance at 450 nm of each well was measured using a microplate reader in triplicate.

2.10. Wound-healing assay

IOSE-80, SKOV3 cells, and lentivirus-transfected SKOV3 cells (2×10^5) (3 replicates per group) were seeded into 6-well plates for scratch assays and incubated until 100 % confluence. A 200-μL pipette tube was utilized to scratch and washed to remove detached cells with serum-free medium, and images of the wound area were taken at 0, 24, 48 and 72 h using a fluorescent inverted microscope. ImageJ software was used to quantify the healing area and the migration rete.

2.11. Transwell assay

The cell invasion ability of cells to invade through Matrigel (40 μL; dilution 1:8; Sigma, St Louis, MO) was assessed using 8.0 nm diameter Matrigel precoated Transwell inserts (Corning, Cambridge, MA). Firstly, cells such as SKOV3 cells (2×10^4 cells) and cells transfected with si-NC, sh-miR-93-5p, ov-NC and ov-miR-93-5p lentivirus were seeded into the upper chamber, then added 10 % serum-complete medium to the lower chamber, and cultured for 24 h in 24-well plates. The chamber was then removed and rinsed in PBS, and the non-invasive cells and Matrigel were wiped off the top surface of the filter using a cotton swab. The inserts were then fixed in methanol for 10 min at room temperature and stained with 0.1 % crystal violet. Cells that migrated to the lower surface were observed and counted in five random fields at a magnification of × 200 under a fluorescence microscope (Olympus, Japan). Each experiment was performed in triplicate and repeated three times.

2.12. Flow cytometry

Annexin V-PE/7-AAD Apoptosis Detection Kit (Yeasen, Shanghai, China) was incubated at room temperature for 10 min in the dark. Then, cells were performed for flow cytometry analysis, washed twice and resuspended in 500 μL buffer, and the results were analyzed with CytExpert software.

2.13. MDA and ROS analysis

Malondialdehyde (MDA) content in cell lysates was determined by a lipid peroxidation assay kit (BC0025, Beijing Solarbio Science

and Technology Co. Ltd, China) on the basis of the instructions. Dihydroethidium (Yeasen Biotechnology Co. Ltd.) was utilized to stain for ROS on a Beckman CytoFLEX flow cytometer (Beckman counlter, CA, USA).

3. Results

3.1. miR-93-5p, ferroptosis was closely related to OC

Firstly, in order to clarify the relationship between ferroptosis and OC, we screened out a number of key genes regulating ferroptosis based on the public database of ferroptosis-related genes, and identified their differential expression in normal tissues and cancer tissues, and found that Driver Genes (genes that promote ferroptosis) such as FTH1, TF, Suppressor genes (suppressing ferroptosis) such as TP53, HMOX1, and ferroptosis-related key genes GSH peroxidase 4 (GPX4), SLC7A11 were differentially expressed, suggesting that ferroptosis played a more or less role in OC (Supplementary Fig. 1). In addition, based on the differential analysis of TCGA mRNA expression profiles, we identified that GPX4 and SLC7A11 were significantly increased in OC, what's more important, and SLC7A11 was differentially higher than GPX4, which was similar with qRT-PCR results (Fig. 1A–D). Furthermore, based on the overall differentially expressed genes, further enrichment analysis results found that cell-to-cell interactions and adhesion were significantly enriched in GO, while KEGG showed that genes were significantly enriched in cell cycle, RAS signaling pathway and cisplatin resistance pathway, which were also closely related to OC (Supplementary Fig. 2A and B).

miR-93-5p, which has been shown to be closely related to a variety of tumors, but its role in OC is still unclear. Therefore, we next aimed to investigate the mechanism of this gene in OC. Based on the public GEO database, we found that the expression of miR-93-5p in OC tissues was significantly lower than that in normal tissues, which was also confirmed by qRT-PCR results (Fig. 1E and F). Subsequently, the enrichment analysis of miR-93-5p and its target genes observed that miR-93-5p was mainly enriched in RAS, NFKB, cell cycle and other pathways (Supplementary Fig. 3A). SLC7A11 is mainly enriched in apoptosis, androgen response, TNFA signaling via NFKB signaling pathway (Supplementary Fig. 3B). Both enrichment results indicated the close relationship between miR-93-5p and SLC7A11. Furthermore, predictions from multiple databases, such as PITA, MIRmap, and microT, all indicated that miR-93-5p had a targeted prediction relationship with SLC7A11. Therefore, miR-93-5p may affect the occurrence and development of OC by down-regulating SLC7A11.

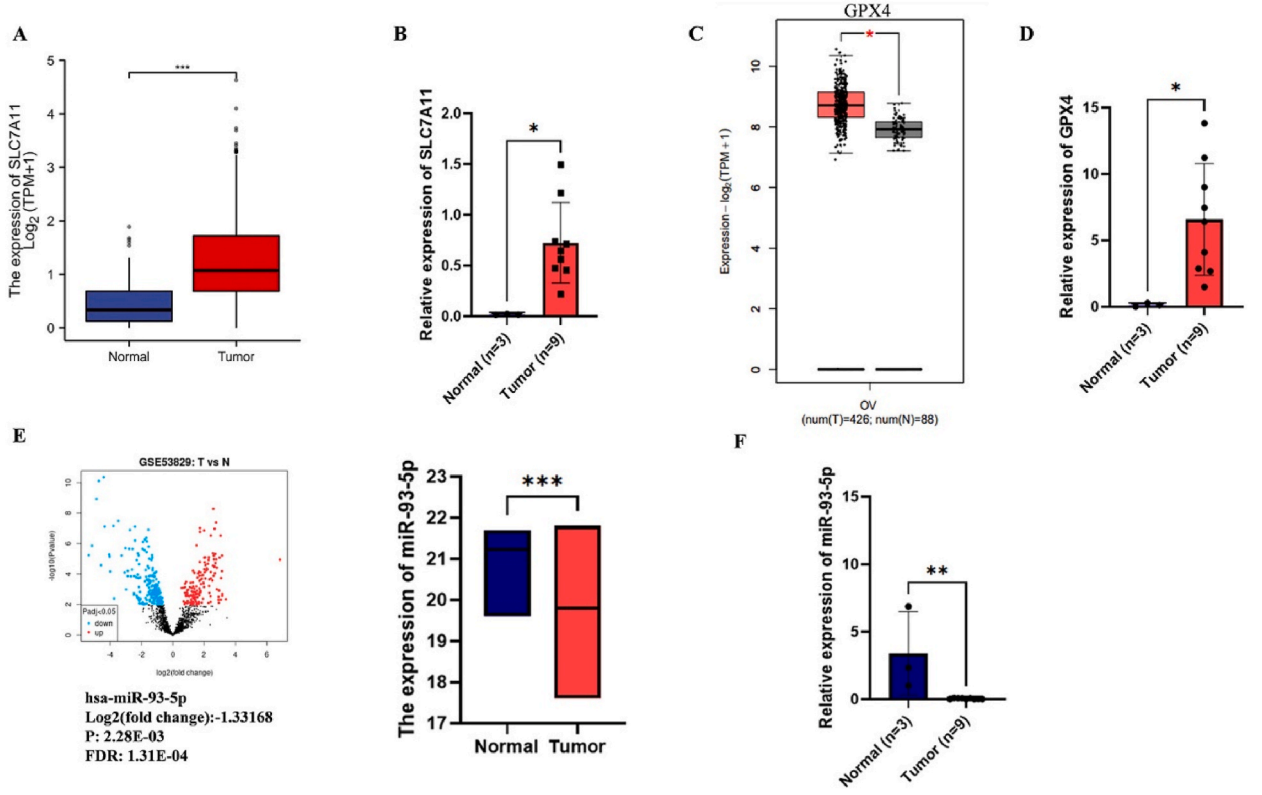

Fig. 1. miR-93-5p, ferroptosis was closely related to ovarian cancer A-B. The differential expression of SLC7A11 between normal and tumor tissues in TCGA database and collected samples C-D. The differential expression of GPX4 between normal and tumor tissues in TCGA database and collected samples E-F. The differential expression of miR-93-5p between normal and tumor tissues in TCGA database and collected samples $P < 0.05$ ("*"), $P < 0.01$ ("**"), $P < 0.001$ ("***").

3.2. Expression of miR-93-5p, SLC7A11 and GPX4 in cell lines

To further verify the above results, we detected the expression of miR-93-5p, SLC7A11 and GPX4 in human normal ovarian cell line IOSE-80 and OC cell line SKOV3. The results of qRT-PCR and Western Blot showed that the mRNA levels and protein expressions of SLC7A11 and GPX4 in SKOV3 cells were higher than those of IOSE-80, while the expression of miR-93-5p was significantly decreased (Fig. 2A and B). Cell behavior experiments demonstrated that OC cells had higher cell proliferation and migration abilities than IOSE-80 (Fig. 2C and D). In addition, the levels of MDA and ROS were significantly up-regulated in SKOV3 compared with IOSE-80, which further indicated that OC was inextricably linked to the state of ferroptosis (Fig. 2E and F).

3.3. The induction of ferroptosis promoted the occurrence of apoptosis in SKOV3 cells

At present, various studies have shown that ferroptosis can inhibit the proliferation of tumor cells in liver cancer, pancreatic cancer, prostate cancer, breast cancer and other cancers, so induction of ferroptosis may be a potential method for the treatment of cancer in the future. Erastin, a class of classic ferroptosis inducers, could prevent extracellular cystine from entering into cells, block the synthesis of intracellular GSH, weaken the antioxidant capacity of cells, and finally lead to the occurrence of ferroptosis by inhibiting System xc-activity. Except for that, Ferrostatin-1 is a potent and selective inhibitor of ferroptosis, which inhibits erastin-induced ferroptosis, preventing damage to membrane lipids through a reducing mechanism, thereby inhibiting cell death. Therefore, we treated SKOV3 cells with erastin and erastin + Fe1 respectively to explore the expression of ferroptosis-related genes and the biological behavior of cells. Excitingly, the Western Blot results showed that the expression of ferroptosis-related key genes SLC7A11 and GPX4 in SKOV3 after erastin treatment for 24 h was significantly decreased, while the expression of SLC7A11 and GPX4 in the erastin + Fe1 treatment group rebounded (Fig. 3A). Meanwhile, CCK8 and flow cytometry detection showed that erastin could significantly restrain the proliferation of cancer cells and promote cell apoptosis. Similarly, Fe-1 could inhibit the effect of erastin to a certain extent (Fig. 3B

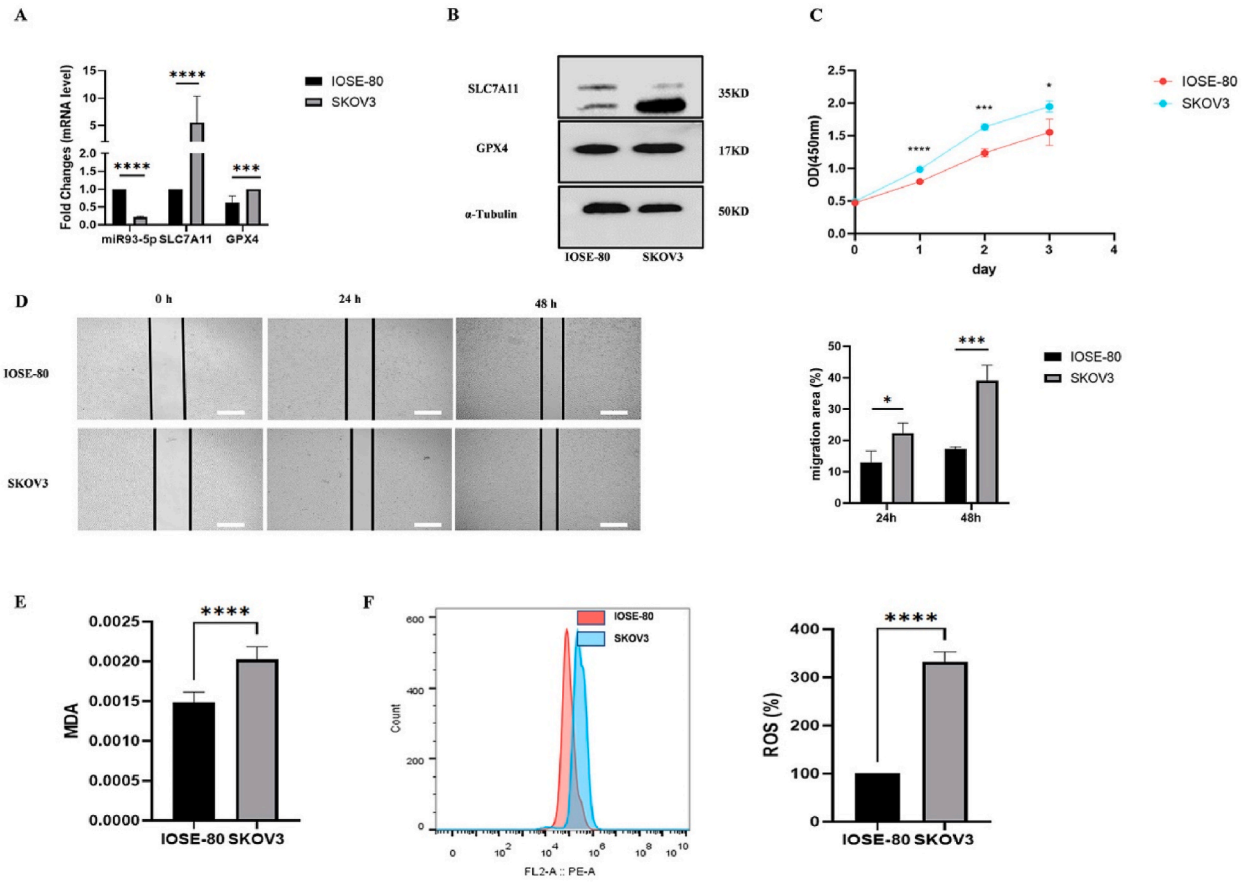

Fig. 2. Expression of miR-93-5p, SLC7A11 and GPX4 in cell lines A. The mRNA expression level of miR-93-5p, SLC7A11 and GPX4 in IOSE-80 and SKOV3 B. The protein expression level of SLC7A11 and GPX4 in IOSE-80 and SKOV3 C. Cell proliferation was detected using CCK8 assay in IOSE-80 and SKOV3 D. The migration ability was detected using wound healing assay in IOSE-80 and SKOV3 E. The content of MDA in IOSE-80 and SKOV3 F. The content of ROS in IOSE-80 and SKOV3 $P < 0.05$ ("*"), $P < 0.01$ ("**"), $P < 0.001$ ("***"). The uncropped version of B has been provided as Supplement file.

and C). The ferroptosis detection indicators MDA and ROS also clearly demonstrated that in OC cells, the use of erastin can significantly promote the production of intracellular MDA and ROS, and induce the occurrence of ferroptosis, while Fe1 can reverse this phenomenon (Fig. 3D and E).

3.4. miR-93-5p regulated malignant phenotype and ferroptosis status of OC

Based on the bioinformatics analysis in the first part, we speculated that miR-93-5p was involved in the malignant biological behavior of OC cells. To elucidate this hypothesis, we first transfected miR-93-5p overexpressing and knockdown lentiviruses in SKOV3 cells, and the transfection efficiency was visualized by fluorescence microscopy (Fig. 4A). Simultaneously, qRT-PCR further verified the transfection efficiency. Next, in order to investigate the effect of miR-93-5p on apoptosis and invasion levels and ferroptosis levels in SKOV3 cells, we first detected the expression of ferroptosis-related key genes SLC7A11 and GPX4 by qRT-PCR and

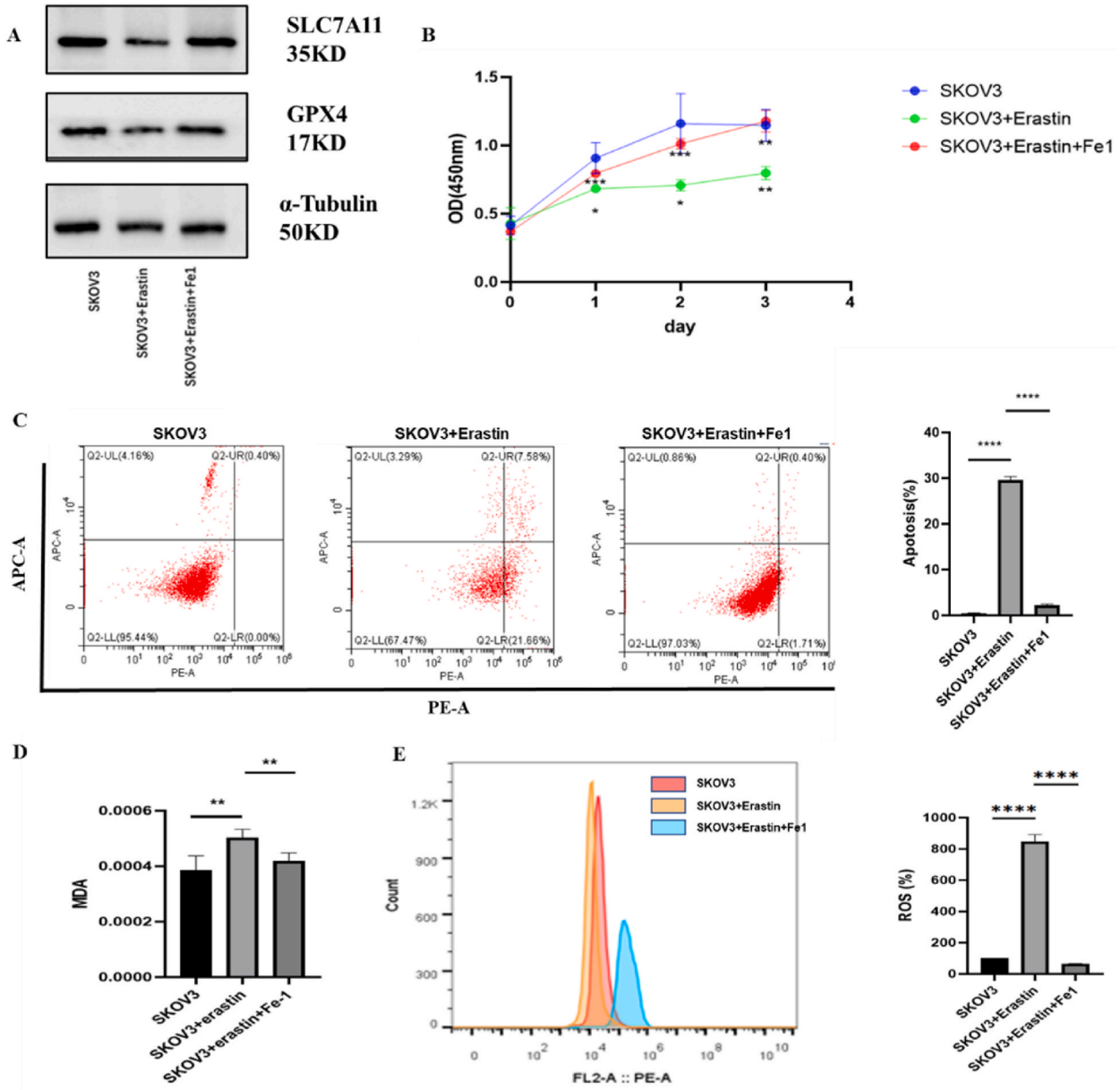

Fig. 3. The induction of ferroptosis promoted the occurrence of apoptosis in SKOV3 cells A. The protein expression level of SLC7A11 and GPX4 in SKOV3 after erastin and Fe1 treatment B. Cell proliferation was detected using CCK8 assay in SKOV3 after erastin and Fe1 treatment C. The apotosis level in SKOV3 after erastin and Fe1 treatment D. The content of MDA in SKOV3 after erastin and Fe1 treatment E. The content of ROS in SKOV3 after erastin and Fe1 treatment P < 0.05 ("*"), $P < 0.01$ ("**"), $P < 0.001$ ("****"). The uncropped version of A has been provided as Supplement file.

Western Blot, and found that overexpression of miR-93–5p could significantly reduce the expression of SLC7A11, which was consistent with the above-mentioned results that the two genes might target each other to regulate the expression. Meanwhile, overexpression of miR-93-5p also significantly increased the expression of BAX and decreased the expression of BCL2, while knockdown of miR-93-5p did the opposite, suggesting that overexpression of miR-93-5p could promote the apoptosis and inhibit the proliferation of SKOV3 cells. In terms of the invasion ability, at the mRNA and protein levels, miR-93-5p could also significantly reduce the expression level of the invasion marker E-cadherin and increase the expression of N-cadherin and Vimentin (Fig. 4B and C). Next, various functional experiments were used to investigate the effect of miR-93-5p on the proliferation and metastasis of SKOV3 cells. The results of CCK8, scratch assay, transwell assay and flow cytometry indicated that overexpression of miR-139-5p significantly reduced cell viability (Fig. 5A), inhibited cell migration and invasion ability, and promoted cell apoptosis (Fig. 5B–D). These results indicated that miR-93-5p as a tumor suppressor gene could inhibit the proliferation, invasion and metastasis of SKOV3 cells. Furthermore, MDA and ROS, as the major process in ferroptosis, showed that overexpression of miR-93-5p led to the accumulation of intracellular ROS and MDA, increasing the level of ferroptosis. Taken together, these results clearly suggested that miR-93-5p played a key role in cell biological phenotype and ferroptosis. More importantly, based on previous findings, we could speculate to some extent that miR-93-5p 5p might

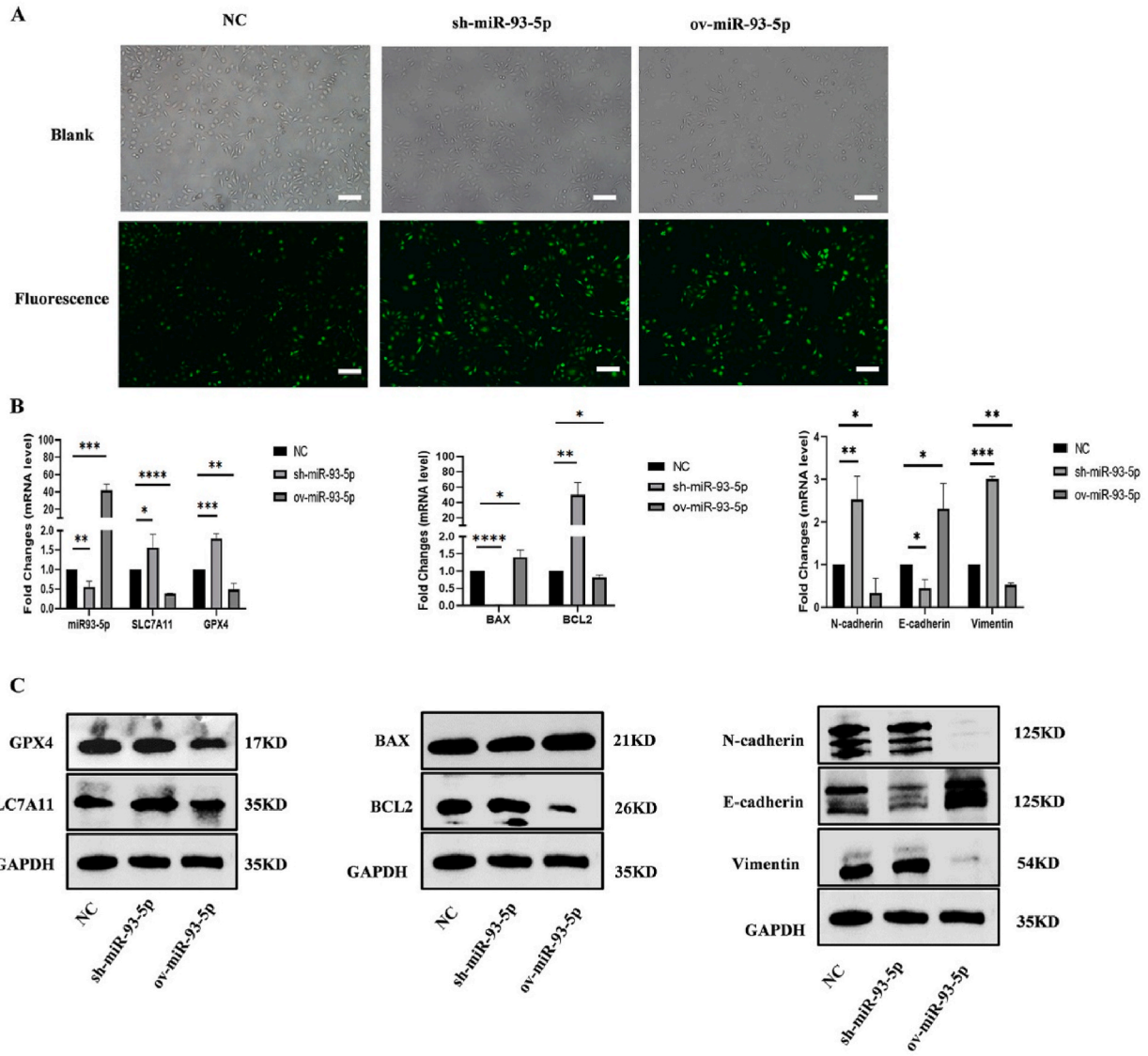

Fig. 4. miR-93-5p regulated malignant phenotype and ferroptosis status of ovarian cancer A. SKOV3 Cells were transfected with NC, sh-miR93-5p and ov-miR93-5p lentivirus B. The mRNA expression level of miR-93-5p, SLC7A11, GPX4 BAX, BCL2, N-cadherin, E-cadherin and Vimentin in NC, sh-miR93-5p and ov-miR93-5p lentivirus groups C. The protein expression level of SLC7A11, GPX4, BAX, BCL2, N-cadherin, E-cadherin and Vimentin in NC, sh-miR93-5p and ov-miR93-5p lentivirus groups $P < 0.05$ ("*"), $P < 0.01$ ("**"), $P < 0.001$ ("***"). The uncropped version of C has been provided as Supplement file.

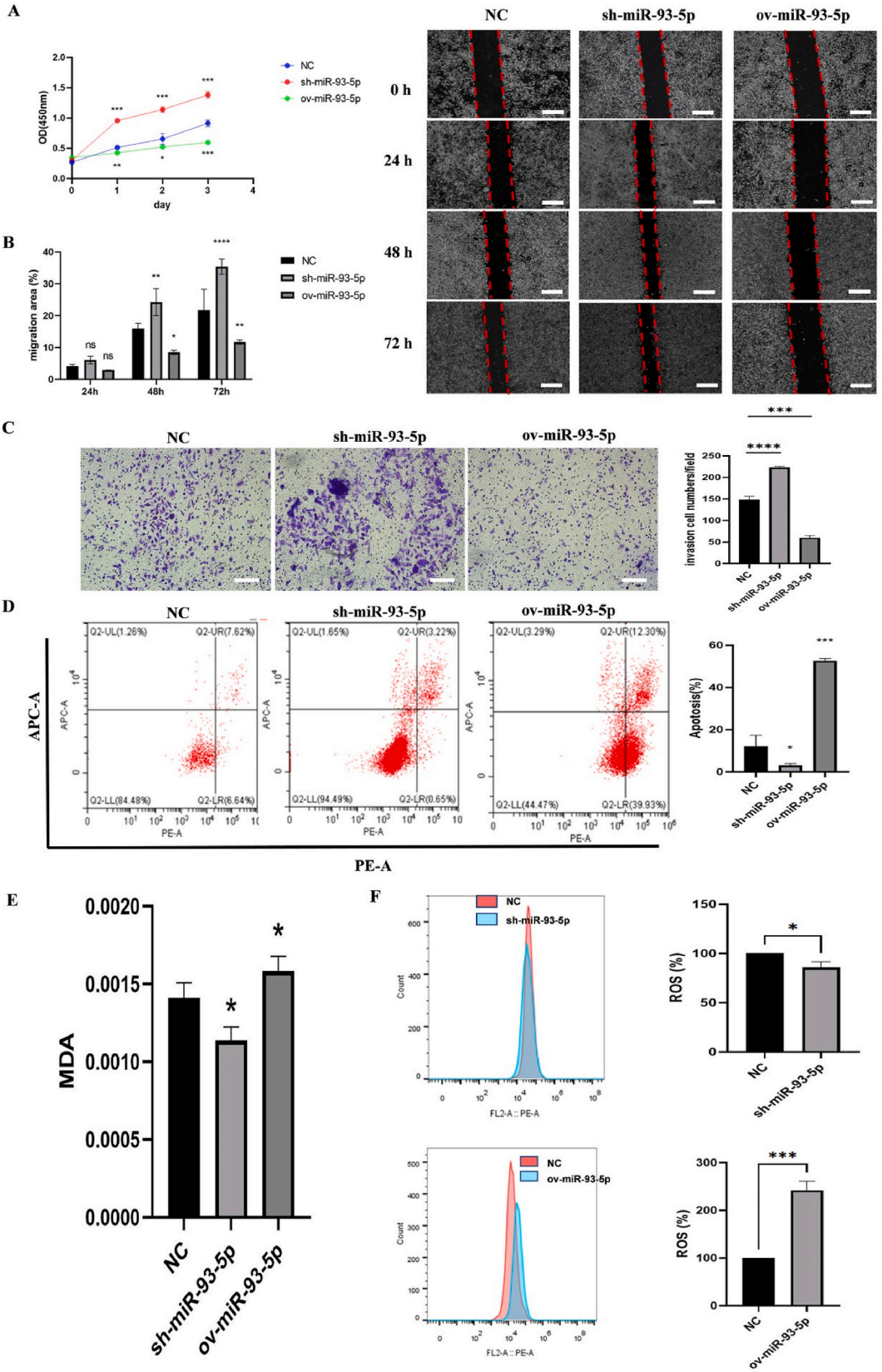

(caption on next page)

Fig. 5. miR-93-5p regulated malignant phenotype and ferroptosis status of ovarian cancer A. Cell proliferation was detected using CCK8 assay in NC, sh-miR93-5p and ov-miR93-5p lentivirus groups B. The migration ability in NC, sh-miR93-5p and ov-miR93-5p lentivirus groups C. The invasion ability in NC, sh-miR93-5p and ov-miR93-5p lentivirus groups D. The apotosis level in NC, sh-miR93-5p and ov-miR93-5p lentivirus groups E. The content of MDA by flow cytometry in the three groups F. The content of ROS by flow cytometry in the three groups $P < 0.05$ ("*"), $P < 0.01$ ("**"), $P < 0.001$ ("***").

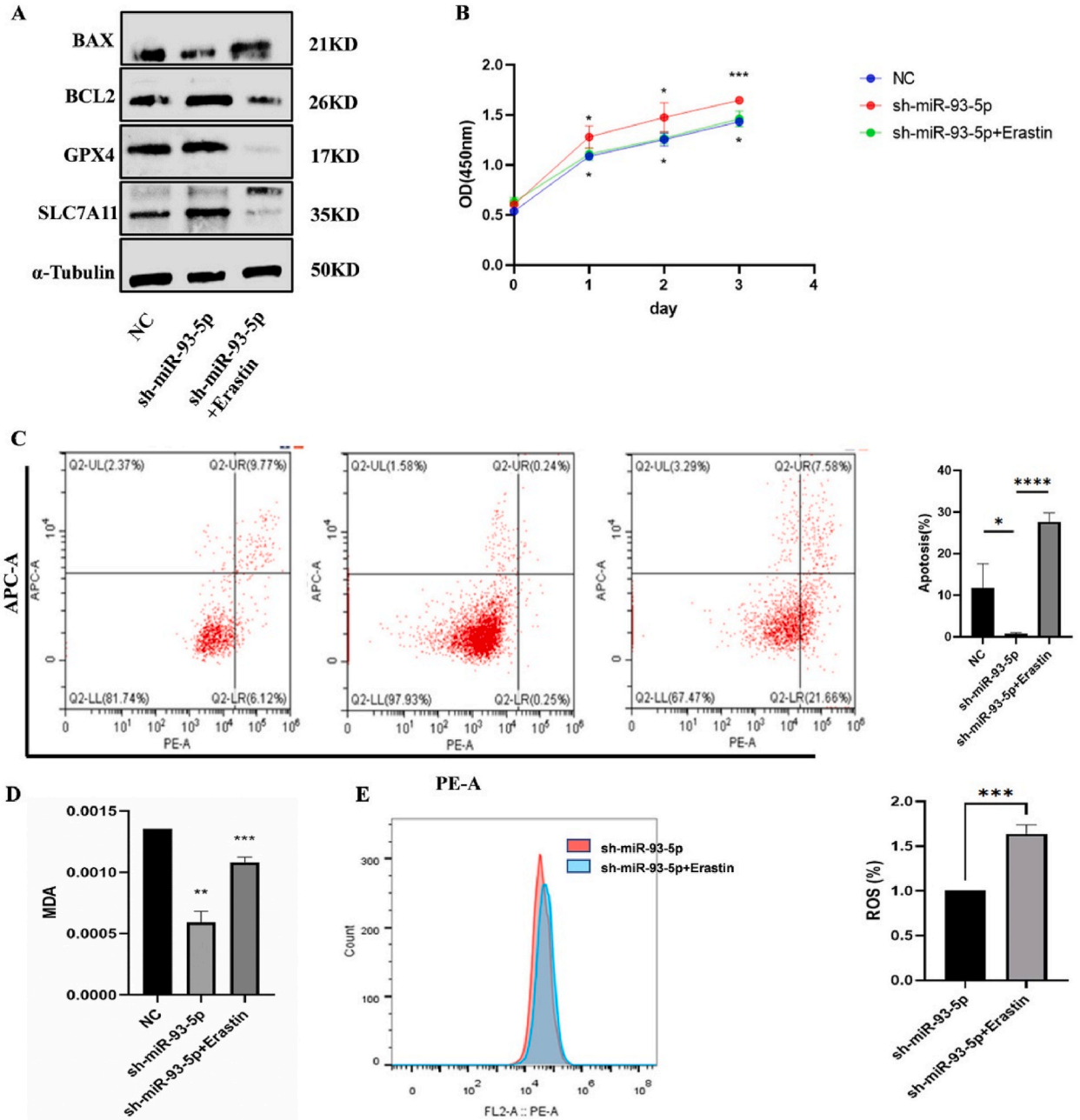

Fig. 6. miR-93-5p regulated ferroptosis by targeting SLC7A11 and then affected cell proliferation and apoptosis A. WB indicated that compared with NC group, SLC7A11, GPX4 and BCL2 were highly expressed in SI group, while erastin could reverse the results B. Cell viability in NC, SI and SI + erastin groups detected by CCK-8 assay C. Flow cytometry assay displayed the apoptosis level in the three groups D. The content of MDA by flow cytometry in the three groups E. The content of ROS by flow cytometry in the three groups $P < 0.05$ ("*"), $P < 0.01$ ("**"), $P < 0.001$ ("***"). The uncropped version of A has been provided as Supplement file.

regulate its expression level by targeting SLC7A11. Besides, SLC7A11, as a key component of the xCT transport system, participated in the transport of intracellular GSH, mediated the occurrence and inhibition of ferroptosis, thus regulating the level of intracellular ferroptosis, ultimately leading to cell biological phenotype changes.

3.5. miR-93-5p regulated ferroptosis by targeting SLC7A11 and then affected cell proliferation and apoptosis

After confirming the anti-tumor function of miR-93-5p, we further studied its specific regulatory mechanism. The above bioinformatics analysis and the results of western blotting and qRT-PCR showed that overexpression of miR-139-5p inhibited the expression of SLC7A11, and the two had the ability to target binding. Therefore, in this part we conducted experiments to verify the above results. Erastin, as a specific drug targeting the xCT system, we used it as an inhibitor of SLC7A11. First, we evaluated at the Western Blot level and found that the expression levels of SLC7A11 and GPX4 were significantly increased in the SI group compared with the NC group, suggesting that knockdown of miR-93-5p would reduce the level of ferroptosis, while the expression of apoptosis-related protein BAX was significantly reduced, while BCL2 significantly increased, which was consistent with previous results. More importantly, the expression of SLC7A11 was significantly decreased in the SI + E group, demonstrating the effect of erastin targeting to inhibit SLC7A11, and the use of erastin also promoted the occurrence of apoptosis (Fig. 6A). Immediately after, when investigating the effect of miR-93-5p targeting SLC7A11 on the proliferation and metastasis of SKOC3 cells, CCK8 and flow cytometry results suggested that inhibition of miR-93-5p significantly enhanced cell proliferation, but when erastin and When knockdown of miR-93-5p co-existed, the cell proliferation ability was significantly reduced (Fig. 6BC). We further found that the levels of MDA and ROS in SI cells after erastin treatment were also significantly increased, which further indicated that miR-93-5p regulated the level of ferroptosis by targeting SLC7A11 and thus affects cell proliferation and apoptosis (Fig. 6DE).

4. Discussion

OC is one of the leading cancers affecting women's health worldwide, which is the fifth leading cause of death among female cancers, after lung, breast, colorectal and pancreatic cancers [20]. In terms of the rapid increase of OC, the Globocan study predicts that by 2035, there will be 371,000 cancer patients and 254,000 deaths [21]. The majority of women with OC are diagnosed with metastatic disease, and these metastases are a primary driver of morbidity and mortality, despite initial sensitivity to chemotherapy [22].

At present, the mainstream treatment for advanced OC is still tumor reduction and chemotherapy, and tumor recurrence occurs in about 70 % of OC patients [23]. Despite current advances in diagnosis and treatment, poor overall survival prognosis remains a major challenge [24]. Therefore, characterization of the underlying molecular mechanism of OC, and exploration of highly sensitive and specific markers are critical for precisely judging the prognosis of patients and carrying out personalized treatment for patients.

Ferroptosis is an iron-dependent form of nonapoptotic cell death, and cell death by ferroptosis has been implicated in diverse processes in cancers [25,26]. Morphological features of ferroptotic cells include changes in mitochondrial structure, as well as nuclear noncontraction and plasma membrane rupture, typically produced by the inhibitory system xc- (ie, erastin) [27]. System xc-, a cystine/glutamate antiporter, imports extracellular cystine in exchange for intracellular glutamate [28]. Deficiency of intracellular cystine induces the decrease of glutathione levels and consequent inactivation of GPX4 function, which leads to accumulating intracellular ROS, thus promoting iron production and cell death [29,30]. Therefore, targeting ferroptosis may be a new therapeutic strategy for OC.

There is increasing evidence that SLC7A11 plays an important role in the progression and survival of different cancers, including breast cancer, glioma, and lung cancer [31–33]. In our study, the expression of SLC7A11 was significantly increased in OC, and the use of the ferroptosis inducer erastin to specifically reduce the expression of SLC7A11 to induce ferroptosis would reverse the malignant phenotypes and inhibition of proliferation in cancer cells, which also indicated that SLC7A11 might function as an oncogene of OC to a certain extent. What's more important, targeting SLC7A11 was likely to be an effective way to mediate ferroptosis, thereby participating in the occurrence and development of tumors. For example, Lidocaine has been reported to promote ferroptosis and inhibit tumor growth in OC by modulating the miR-382-5p/SLC7A11 axis [34], which further illustrated the important role of SLC7A11-involved ferroptosis in the occurrence and development of OC.

At present, a large number of studies have shown that miRNAs are important regulators of OC progression, and the abnormal expression of miRNAs can be used as prognostic indicators for OC therapeutic targets. miR-93-5p, has been shown to be involved in regulation in a variety of tumors. For example, Yang et al. found that overexpression of miR-93-5p significantly promoted the proliferation, invasion and migration of prostate cancer cells and other malignant phenotypes, which functioned as a prognostic gene in prostate cancer [15]. Not only that, miR-93-5p was also highly expressed in cervical cancer tissues and cells, and its high expression predicted a poor prognosis. Further experiments found that overexpression of miR-93-5p could significantly promote cancer cell growth, proliferation, invasion and migration by reducing the expression of THBS2 [35]. Nevertheless, the research and finding of miR-93-5p in OC is still unclear. A previous study found that the expression of miR-93 in OC and borderline tumors was significantly lower than that in normal ovarian tissue, and tumor growth was inhibited by reducing the expression of RhoC [36]. In our study, the expression of miR-93-5p in cancer tissues and cancer cells was significantly lower than that in the normal group, and overexpression of miR-93-5p could significantly inhibit the proliferation, migration and invasion of SKOV3 cells, suggesting that this gene acted as a tumor suppressor in OC and suppressed the development of OC.

Surprisingly, through multiple bioinformatics prediction platforms, we found that SLC7A11 is a potential target of miR-93-5p, and overexpression of miR-93-5p can significantly reduce the expression of SLC7A11 and inhibit the malignant biological behavior and promote ferroptosis in SKOV3 cells, whereas knockdown of miR-93-5p does the opposite. Not only that, the use of erastin on the basis

of knockdown of miR-93-5p can significantly reverse the malignant phenotype. Therefore, considering the binding relationship between miR-93-5p and SLC7A11, miR-93-5p may promote ferroptosis and inhibit OC progression by directly targeting and down-regulating SLC7A11. Overall, miR-93-5p plays an important role in ferroptosis and tumor malignant phenotype. As a tumor suppressor gene in OC, it may be a new and promising target for OC in the future. The miR-93-5p-SLC7A11 axis regulates the occurrence and development of OC through ferroptosis and also provides a new direction for the diagnosis and treatment of OC.

Ethics statement

The utilization of human subjects in our research was subject to review and approval by the Renmin Hospital Research and Ethics Committee (WDRY2020-K218).

Patient consent for publication

Not applicable.

Funding

This research was financially supported by the National Natural Science Foundation of China (82071655, 81860276); Research on Nursing for Nasal High-Frequency Humidified Oxygen Therapy After Gynecological Laparoscopic Surgery (WX21C12).

Data availability statement

Data will be made available on request. Data associated with your study has not been deposited into a publicly available repository.

CRediT authorship contribution statement

Zitao Wang: Writing – review & editing, Writing – original draft. **Xiao Yang:** Formal analysis, Data curation. **Yanqing Wang:** Investigation, Formal analysis. **Hua Liu:** Writing – review & editing. **Yanxiang Cheng:** Validation.

Declaration of competing interest

The authors declare that they have no known competing financial interests or personal relationships that could have appeared to influence the work reported in this paper.

Acknowledgments

Not applicable.

Abbreviations

OC	Ovarian cancer
ROS	reactive oxygen species
SLC7A11	Solute carrier family 7 member 11
miRs	MicroRNAs
qRT-PCR	Quantitative real-time PCR
CCK-8	Cell Counting Kit-8 assay
FACS	Fluorescence-activated cell sorting
MDA	Malondialdehyde
GPX4	GSH peroxidase 4
DEGs	differentially expressed gene

Appendix A. Supplementary data

Supplementary data to this article can be found online at https://doi.org/10.1016/j.heliyon.2024.e35457.

References

[1] P.H. K, R.J. J, C.M. L, Recent trends in ovarian cancer incidence and relative survival in the United States by race/ethnicity and histologic subtypes, Cancer Epidemiol. Biomarkers Prev. : a publication of the American Association for Cancer Research, cosponsored by the American Society of Preventive Oncology 26 (10) (2017).
[2] T.L. A, T. Britton, D.C. E, M.K. D, S. Goli, R.C. D, G.M. M, J. Ahmedin, S.R. L, Ovarian cancer statistics, 2018, J] CA: a cancer journal for clinicians 68 (4) (2018).
[3] W.S. Hambright, R.S. Fonseca, L. Chen, R. Na, Q. Ran, Ablation of ferroptosis regulator glutathione peroxidase 4 in forebrain neurons promotes cognitive impairment and neurodegeneration, Redox Biol. 12 (2017).
[4] L. Chen, Z. Xinglin, Y. Mengsu, D. Xiaochen, Recent progress in ferroptosis inducers for cancer therapy, Advanced materials (Deerfield Beach, Fla.) 31 (51) (2019).
[5] Y. Yang, F. Qi, H. Jianyun, W. Yaoqiu, L. Haiyan, Z. Qingxue, Ferroptosis-related gene signature promotes ovarian cancer by influencing immune infiltration and invasion, Journal of Oncology (2021) (PP. 9915312–9915312).
[6] Y. Bing, L. Feng, S. ZhiZhou, R. Yuan, D. XiaoLi, Y. TingTing, L. DengYuan, L. RuFang, P. DanDan, W. YuJue, T. Yan, Y. Zhen, Z. YunHui, Dihydroartemisinin inhibits the proliferation, colony formation and induces ferroptosis of lung cancer cells by inhibiting PRIM2/slc7a11 Axis,[J], OncoTargets Ther. 13 (2020).
[7] L. Pengfei, F. Yetong, L. Hanwei, C. Xin, W. Guangsuo, X. Shiyuan, L. Yalan, Z. Lei, Ferrostatin-1 alleviates lipopolysaccharide-induced acute lung injury via inhibiting ferroptosis, Cell. Mol. Biol. Lett. 25 (7) (2020).
[8] W. Yadong, S. Xiangjie, S. Bin, Q. Xiaoling, Z. Jianjiang, MiR-375/SLC7A11 axis regulates oral squamous cell carcinoma proliferation and invasion, Cancer Med. 6 (7) (2017).
[9] S. Christina, I. Rouzanna, Z. Christoph, S. Theresa, R. Franziska, H. Lynette, G. Florian, V. Beate, F.M. Carolina, M. Nicole, T. Anna, P. Áine, W. Alina, P. Charlotta, G. Sandra, G.K. S, G. Jochen, D.D. C, M. Steffen, E. Marieke, W. Claudia, G. Hartmut, S. Mathias, P. Christian, E. Wolfgang, O.R.A. J, Niche WNT5A regulates the actin cytoskeleton during regeneration of hematopoietic stem cells, J. Exp. Med. 214 (1) (2017).
[10] S. R, B. B, P. S-M, P.M. E, MicroRNAs: key players in the immune system, differentiation, tumorigenesis and cell death, Oncogene 27 (45) (2008).
[11] Z. Huilin, L. Bingjian, microRNAs as biomarkers of ovarian cancer, Expet Rev. Anticancer Ther. 20 (5) (2020).
[12] L. Li, H. Gu, L. Chen, P. Zhu, L. Zhao, Y. Wang, X. Zhao, X. Zhang, Y. Zhang, P. Shu, Integrative network analysis reveals a MicroRNA-based signature for prognosis prediction of epithelial ovarian cancer, BioMed Res. Int. 2019 (2019).
[13] Y. Meng, X. Ran, W. Xinru, X. Youyi, D. Zhenfeng, L. Duolu, K. Quancheng, MiR-93-5p regulates tumorigenesis and tumor immunity by targeting PD-L1/CCND1 in breast cancer, Ann. Transl. Med. 10 (4) (2022).
[14] S. Xuan, L. Tao-Tao, Y. Xiang-Nan, B. Asha, Z. Hai-Rong, G. Hong-Ying, Z. Guang-Cong, B. Enkhnaran, S. Jia-Lei, S. Guang-Qi, W. Shu-Qiang, D. Ling, O. Michael, Z. Ji-Min, S. Xi-Zhong, microRNA-93-5p promotes hepatocellular carcinoma progression via a microRNA-93-5p/MAP3K2/c-Jun positive feedback circuit, J] Oncogene 39 (35) (2020).
[15] Y. Yuemei, J. Binghan, Z. Xiaoling, W. Yao, Y. Weiliang, miR-93-5p may be an important oncogene in prostate cancer by bioinformatics analysis, J. Cell. Biochem. 120 (6) (2019).
[16] L. Li, J. Zhao, S. Huang, Y. Wang, L. Zhu, Y. Cao, J. Xiong, J. Deng, MiR-93-5p promotes gastric cancer-cell progression via inactivation of the Hippo signaling pathway, Gene 641 (2018).
[17] G. Ahmed, P. Dunfa, C. Zheng, S. Mohammed, A. Khaled, C. Alejandro, E.-R. Wael, Epigenetic regulation of AURKA by miR-4715-3p in upper gastrointestinal cancers, Sci. Rep. 9 (1) (2019).
[18] Z. Kexin, W. Longfei, Z. Peng, L. Meiying, D. Jing, G. Tongtong, O.C. Douglas, W. Gaoyang, W. Hong, Y. Yongfei, miR-9 regulates ferroptosis by targeting glutamic-oxaloacetic transaminase GOT1 in melanoma, Mol. Carcinog. 57 (11) (2018).
[19] L. Meiying, W. Longfei, Z. Kexin, W. Hong, Z. Tian, G. Lucas, O.C. Douglas, Z. Peng, L. Yu, G. Tongtong, R. Wenyan, Y. Yongfei, miR-137 regulates ferroptosis by targeting glutamine transporter SLC1A5 in melanoma, Cell Death Differ. 25 (8) (2018).
[20] S.R. L., M.K. D., F.H. E., J. Ahmedin, Cancer statistics, 2021,[J], CA A Cancer J. Clin. 71 (1) (2021).
[21] S. Hyuna, F. Jacques, R.L. S, L. Mathieu, S. Isabelle, J. Ahmedin, B. Freddie, Global cancer statistics 2020: GLOBOCAN estimates of incidence and mortality worldwide for 36 cancers in 185 countries, J] CA: A Cancer Journal for Clinicians 71 (3) (2021).
[22] A.L. Carlton, A. Illendula, Y. Gao, D.C. Llaneza, A. Boulton, A. Shah, R.A. Rajewski, C.N. Landen, D. Wotton, J.H. Bushweller, Small molecule inhibition of the CBFβ/RUNX interaction decreases ovarian cancer growth and migration through alterations in genes related to epithelial-to-mesenchymal transition, Gynecol. Oncol. 149 (2) (2018).
[23] O. Brian, E.R. P, Diagnosis and treatment of ovarian cancer, Hematol. Oncol. Clin. N. Am. 32 (6) (2018).
[24] E.E. A, Real-world evidence in the treatment of ovarian cancer,[J] Annals of oncology, official journal of the European Society for Medical Oncology 28 (suppl_8) (2017).
[25] P. Koppula, L. Zhuang, B. Gan, Cystine transporter SLC7A11/xCT in cancer: ferroptosis, nutrient dependency, and cancer therapy, Protein & cell 12 (8) (2020).
[26] M. Yanhua, W. Jun, W. Jinchun, H. Dan, Z. Chunfang, D. Chaojun, L. Bin, Ferroptosis, a new form of cell death: opportunities and challenges in cancer, J. Hematol. Oncol. 12 (1) (2019).
[27] H. Liuqing, Z. Wei, C. Quan, Y. Yishu, W. Yixuan, W. Junpu, W. Xiaoying, Ovarian cancer cell-secreted exosomal miR-205 promotes metastasis by inducing angiogenesis, J] Theranostics 9 (26) (2019).
[28] L. Maisie, W. Yu-Zhuo, G.P. W, The x(c)- cystine/glutamate antiporter: a potential target for therapy of cancer and other diseases, J. Cell. Physiol. 215 (3) (2008).
[29] J. Jie, S. YaNan, W. Kun, Mechanism of ferroptosis: a potential target for cardiovascular diseases treatment, Aging and disease 12 (1) (2021).
[30] C.J. Yinuo, D.S. J, Mechanisms of ferroptosis, Cell. Mol. Life Sci. : CMLS 73 (11–12) (2016).
[31] Y. Poonam, S. Priyanshu, S. Sandhya, V. Ganesh, B.A. Kanti, K. Devarajan, SLC7A11/xCT is a target of miR-5096 and its restoration partially rescues miR-5096-mediated ferroptosis and anti-tumor effects in human breast cancer cells, Cancer Lett. 522 (2021).
[32] J. Xiangming, Q. Jun, R.S.M. Jamshedur, S.P. J, Z. Yong, H.B. K, H.M. D, T.I. A, H. Chen, E. Rosana, R.J. C, Y.J. D, M.P. P, xCT (SLC7A11)-mediated metabolic reprogramming promotes non-small cell lung cancer progression, Oncogene 37 (36) (2018).
[33] Z. Xinde, Z. Ming, Y. Yong, L. Minjie, The ubiquitin hydrolase OTUB1 promotes glioma cell stemness via suppressing ferroptosis through stabilizing SLC7A11 protein, Bioengineered 12 (2) (2021).
[34] S. Dan, L.Y. Chun, Z.X. Yu, Lidocaine promoted ferroptosis by targeting miR-382-5p/SLC7A11 Axis in ovarian and breast cancer, Front. Pharmacol. 12 (2021).
[35] S. X-Y, H. X-M, Z. X-L, C. X-M, Z. Y, MiR-93-5p promotes cervical cancer progression by targeting THBS2/MMPS signal pathway, Eur. Rev. Med. Pharmacol. Sci. 23 (12) (2019).
[36] C. Xi, C. Shuo, X. Yin-Ling, S. Kai-Xuan, Z. Zhi-Hong, Z. Yang, RhoC is a major target of microRNA-93-5P in epithelial ovarian carcinoma tumorigenesis and progression, Mol. Cancer 14 (1) (2015).